



<https://doi.org/10.11646/mesozoic.1.3.20>

<http://zoobank.org/urn:lsid:zoobank.org:pub:FC189EB8-F494-4D3C-9850-D9D8CD7100A6>

The depositional differences of confined and unconfined turbidite sheet systems

QUN LIU^{§,*} & XIANG-YANG JI[§]

School of Environmental Sciences, Nanjing Xiaozhuang University, Nanjing 211171, China

✉ Qunliu2019@hotmail.com; <https://orcid.org/0000-0001-5884-5645>

✉ jxysgtc@outlook.com; <https://orcid.org/0009-0008-8006-8772>

[§]Contributed equally to this work

*Corresponding author

Abstract

The depositional architecture between unconfined and confined turbidite sheet systems are increasingly recognized, but the major differences are not summarized. This paper aims to summarize the major differences based on the well-studied published systems with known degree of confinement and depositional architectures. The unconfined and confined turbidite sheet systems differ greatly in four aspects: sedimentary facies, stacking patterns of individual beds, facies associations and onlap styles. The sedimentary facies in confined systems are mainly thick beds, occasionally with grain size breaks, overlain by thick mud caps; whereas beds in unconfined turbidite systems present less mud proportion. The stacking patterns in confined systems are mainly vertically stacked, whereas compensationally stacked in strike direction, and progradationally or retrogradationally stacked in dip direction. One facies association has only been identified in confined systems and four facies associations are found in unconfined systems. The vertical log of unconfined turbidite sheet systems presenting a transition of facies association, whereas no transitions in confined systems. The depositional architecture of turbidite sheet systems is controlled by both sediment supply and basin relief. The establishment between degree of confinement and various parameters in this study can be applied in the petroleum industry.

Keywords: degree of confinement, depositional architecture, stacking pattern, controlling factors

Introduction

Turbidite sheet sandstone bodies developed at the terminus of a submarine channel (Fig. 1) may either be unconfined and exhibit a lobate shape, as observed by side scan sonar or in 3D seismic (Gervais *et al.*, 2006; Deptuck *et al.*, 2008; Jegou *et al.*, 2008; Dennielou *et al.*, 2017) or

be confined and process a basin-correspondent planform geometry across the depocentre (Lucchi & Valmori, 1980; Weaver *et al.*, 1992; Wynn *et al.*, 2002; Amy & Talling, 2006). A generic depositional model of turbidite sheet systems has not previously been established. In confined turbidite sheet systems, individual turbidity currents are efficient enough to reach the basin margin and systems are built up by the vertical stacking of individual beds (Lucchi & Valmori, 1980; Weaver *et al.*, 1992; Wynn *et al.*, 2002; Remacha & Fernandez, 2003; Amy & Talling, 2006; Stevenson *et al.*, 2013). However, in unconfined turbidite sheet systems, individual turbidity currents are not big enough to reach the basin margin and systems are built up by compensational stacking of individual beds (Dudley *et al.*, 2000; Prélat *et al.*, 2009; Marini *et al.*, 2015). In this manuscript, the term “turbidite sheet systems” is used in a broader sense, encompassing sand bodies developed at the terminus of both unconfined and confined systems. In contrast, the term “submarine lobe” implies a lobate shape and is applicable exclusively to unconfined systems.

Flow efficiency has been defined as the ability of sediment gravity flow to carry sand in a basinward direction (Mutti, 1977, 1978). Mutti (1978) further expanded the concept of flow efficiency to incorporate also the ability of the flow to segregate its grain populations into distinct facies types with distance. It thus plays a major role in determining the location and geometry of sand deposited from turbidity currents. Factors determining the efficiency of turbidity currents have been discussed by several authors (*e.g.*, Mutti 1992; Mutti & Normark 1987; Normark & Piper 1991; Liu *et al.*, 2018a). Very highly efficient flows will fully segregate the grain populations contained within the parental flow with distance, thus producing relatively well-sorted facies types. Conversely, very poorly efficient flows will only partly segregate their different grain populations, thus producing a more limited

number of facies types characterized by poor textural sorting.

Implicit in the concept of confinement is the relationship of flow efficiency to the size of the depocentre and it has previously only been qualitatively described (Mutti & Lucchi, 1978; Lomas & Joseph, 2004; Kneller *et al.*, 2016). Four types of confinement have been proposed depending on whether sediment reaches the basin margins and the extent of its interaction with the margins. When a flow reaches all margins of a basin, it is referred to as ponded; when only one side of the basin is reached, it is referred to as laterally or frontally confined depending on the entry point of the turbidity currents. When no contact with the basin margin occurs, it is referred to as unconfined (Figs 1, 2; Tórkés & Patacci, 2018).

This study analyses the sedimentary characteristics of more than twenty well-studied published confined and unconfined turbidite sheet systems. It aims to 1) summarize the key differences between these two systems; and 2) establish proxies that can indicate degree of confinement, thereby helping to infer depositional architecture.

Material and methods

Nearly twenty well-studied confined and unconfined turbidite sheet systems have been chosen in this study and their main characteristics (sedimentary facies, facies associations, stacking patterns and depositional architectures) been summarized. The main confined systems are: Miocene Marnoso Arenacea Formation of the Italian Apennines; Oligocene Peira Cava Sandstones, France; Early Miocene Costa Grande member; Crognaleto complex, the Southern Laga Basin, Italy; the

main unconfined systems are Fan 2, 3, Tanqua Karoo, Africa; Stage II, Cerro Bola; Mt. Bilanciere complex, the Southern Laga Basin, Italy; Palaeogene Zheya Formation, Saga area, South Tibet. The large dataset could capture a wide range of basin size and flow efficiency, which adds the variety of turbidite sheet systems.

Results

The comparisons between unconfined and confined turbidite sheet systems are focused on four aspects: sedimentary facies, stacking patterns, facies associations, and controlling factors, all of which will be discussed in detail in the following sections.

Sedimentary facies

Sedimentary facies refer to bodies of sedimentary rock with specific physical, chemical and biological characteristics (Mutti, 1977). In sedimentary gravity flow deposits, the scale of individual facies matches the scale of single flow deposits. Turbidite facies are significantly different between highly confined and unconfined turbidite sheet systems in this study due to different degree of confinement, *i.e.*, the degree of interaction with the basin margin. The common facies recognized in unconfined systems are: (F1) normally graded sandstone with convoluted top; (F2) structureless sandstone with pipes and dish structures; (F3) normally graded sandstone with mud-clast rich top; (F4) structureless sandstone with granule lags; (F5) parallel laminated sandstone with scattered mudstone clasts; (F6) parallel laminated passing upwards into rippled sandstone with a centimetre-scale

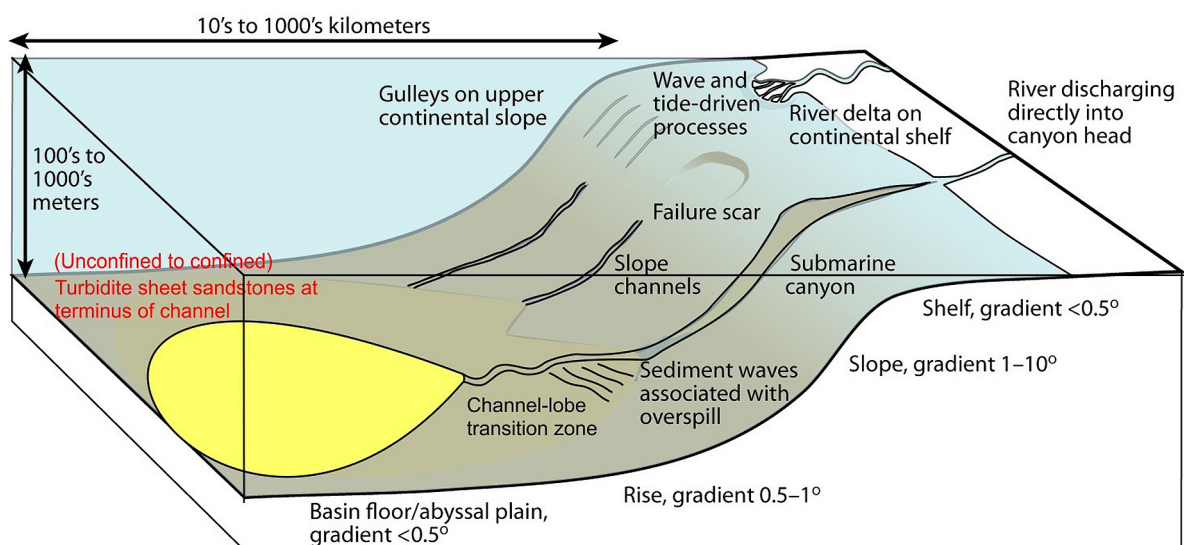


FIGURE 1. The physiography of continental margin illustrating the shelf, slope and basin floor environment. This study focuses on basin floor turbidite sheet sandstone systems (modified from Meiburg & Kneller, 2010).

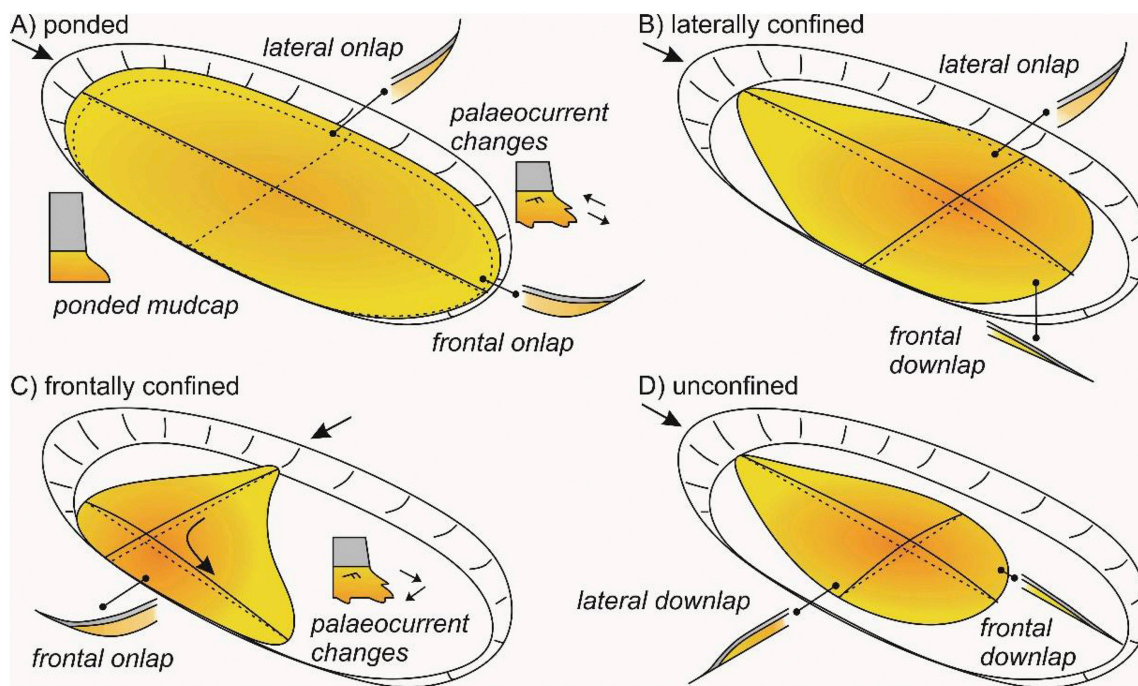


FIGURE 2. Four types of confinement. **A,** Pounded. **B,** Laterally confined. **C,** Frontally confined. **D,** Unconfined (Tökés & Patacci, 2018).

TABLE 1. Summarised stacking patterns in various turbidite sheet systems.

Turbidite sheet systems (cited literature)	Stacking patterns
Quaternary Zaire Fan, offshore Congo (Babonneau <i>et al.</i> , 2002; Picot <i>et al.</i> , 2016); Carboniferous Ross Sandstone Formation, Ireland (MacDonald <i>et al.</i> , 2011); Eocene Central Basin of Spitsbergen (Grundvåg <i>et al.</i> , 2014).	Progradational
Latest Pleistocene Golo fan system, offshore East Corsica, France (Gervais <i>et al.</i> , 2006; Deptuck <i>et al.</i> , 2008); Pleistocene basin-floor, offshore Borneo, Indonesia (Saller <i>et al.</i> , 2008); Fan 3, Tanqua depocentre, Karoo basin, South Africa (Prélat <i>et al.</i> , 2009); Unit A of the Permian Laingsburg Formation, South Africa (Spsychala <i>et al.</i> , 2017b).	Compensational
Rhone Neofan (Jegou <i>et al.</i> , 2008).	Retrogradational
Peira cava, France (Amy <i>et al.</i> , 2007), Marnoso Arenacea Formation, Italy (Amy & Talling, 2006); 'Confined lobes' of Lower Messinian Laga Basin Central Apennines, Italy (Marini <i>et al.</i> , 2015); Eocene Hecho Group, Spain (Remacha <i>et al.</i> , 2005).	Aggradation

mudstone cap; (F7) ripple-cross laminated sandstone to mudstone top. Three common facies are recognized in confined turbidite sandstones: (F8) alternation of parallel- and ripple-laminated sandstone to siltstone and mudstone; (F9) structureless sandstone passing upwards into thick mudstone top; (F10) Bouma-like package overlain by multiple massive sandstone overlain by mudstone top, sharp grain size breaks at the boundary (Representative photos are shown in Figs 3, 4).

Stacking patterns

Stacking patterns are mainly controlled by the degree of confinement, avulsion of the feeder-channels and sediment supply (Spsychala, 2017b, Terlaký *et al.*, 2016). In general, four types of stacking pattern have been disclosed in unconfined turbidite sheet systems: compensational, progradational and retrogradational (Table 1) (Babonneau *et al.*, 2002; Gervais *et al.*, 2006; Deptuck *et al.*, 2008; Saller *et al.*, 2008; Prélat *et al.*, 2009; Grundvåg *et al.*, 2014; Picot *et al.*, 2016; Spsychala











Main sedimentary facies occurred in unconfined turbidite sheet system		Main sedimentary facies occurred in confined turbidite sheet system	
F1	 Normally graded sandstone with convoluted top	F8	 Alternation of parallel- and ripple-laminated sandstone to siltstone and mudstone cap
F2	 Structureless sandstone with pipes and dish structures	F9	 Structureless sandstone passing upwards into thick mudstone top
F3	 Normally graded sandstone with mud-clast rich top	F10	 Bouma-like package overlain by multiple massive sandstone overlain by mudstone top, sharp grain size breaks at the boundary
F4	 Structureless sandstone with granule lags		
F5	 Parallel laminated sandstone with scattered mudstone clasts		
F6	 Parallel laminated passing into ripple-cross laminated sandstone with mudstone cap		
F7	 Ripple-cross laminated sandstone to mudstone top		

FIGURE 3. Main sedimentary facies recognized in unconfined and confined turbidite sheet systems (Weaver *et al.*, 1992; Talling *et al.*, 2007a; Spychala *et al.*, 2017a; Liu *et al.*, 2018a, 2021b).

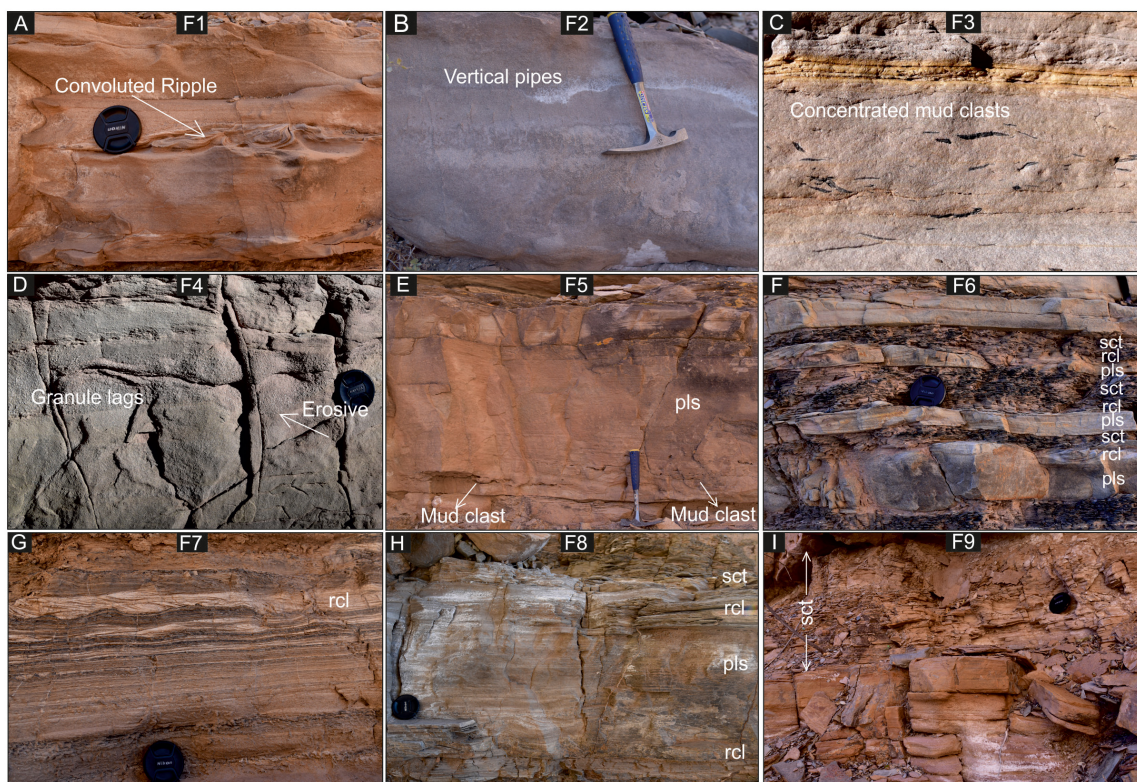


FIGURE 4. Main sedimentary facies recognized in unconfined and confined turbidite sheet systems. The description of the facies is given in Fig. 3. pls, parallel laminated sandstone; sct, siltstone and claystone; rcl, ripple cross lamination (Liu *et al.*, 2018b).

et al., 2017b) and aggradation stacking has been disclosed in confined settings (Haughton 1994; Remacha *et al.*, 2005; Amy & Talling, 2006; Marini *et al.*, 2015). Overlap

index (OI) as a parameter to quantify stacking patterns have been established (Fig. 5). It is represented by $OI = A0/A1$, where A0 is the overlap area and A1 is the area

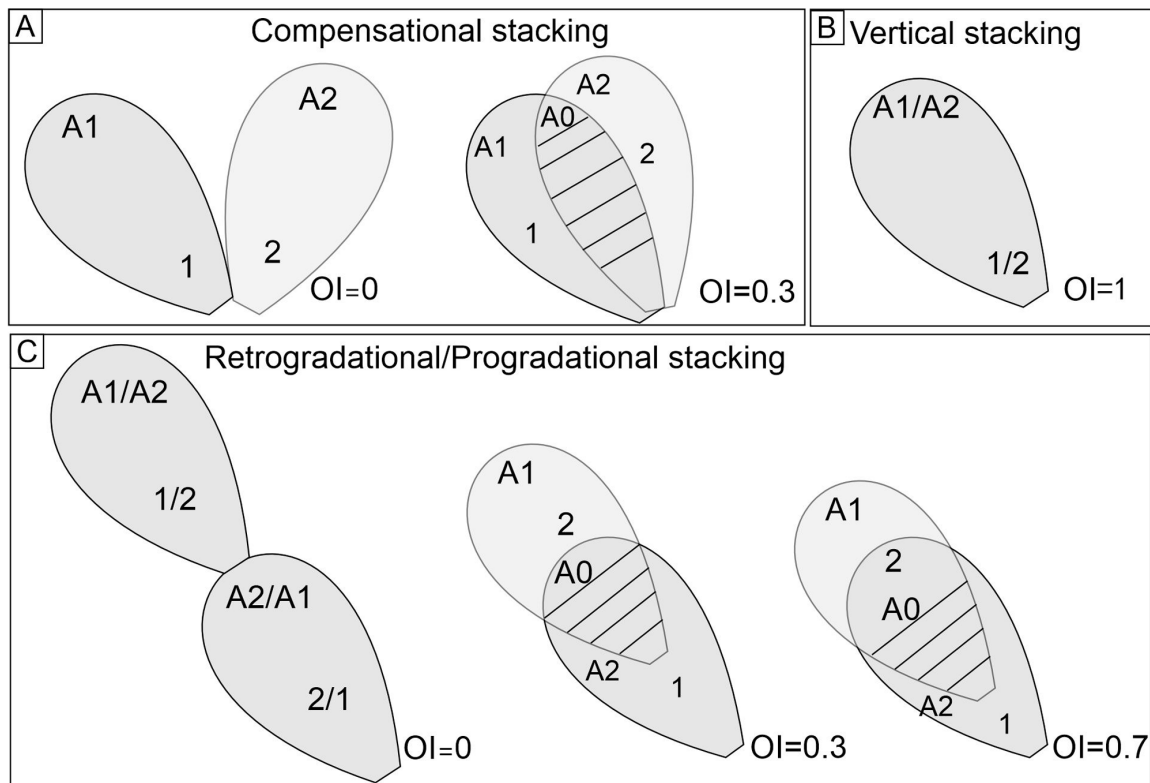


FIGURE 5. Overlap index used to quantify stacking patterns. Cartoon showing the specific overlap index (OI) (OI= 0, 0.3, 1) of two depositional elements (A1 and A2) and their possible stacking patterns. OI is represented by $OI= A0/A1$, where A0 is the overlap area and A1 is the area of older depositional element (Liu *et al.*, 2018b).

of the older depositional element. By estimating the overlap index values of depositional elements in each depositional system, we seek to establish a relationship between overlap index and degree of confinement.

Compensational stacking patterns exhibit a tendency for sediment gravity flows to fill the topographic lows created by preceding deposits (Mutti & Sonnino, 1981). A process-based numerical model has shown the interplay between unconfined turbidity current and preceding deposits, resulting in a subtle and evolving depositional topography, determining the loci of deposition of subsequent flows (Groenenberg *et al.*, 2010). Deptuck *et al.* (2008) observed systematic shifts in the locus of the thickest deposits at the bedding scale due to the subtle morphological influence of preceding deposits on the trajectory of succeeding flows in the turbidite sheet systems of the Golo system, offshore East Corsica. At lobe scale, the compensation has been achieved by avulsion of distributary channels that fed the lobes (Gervais *et al.*, 2006; Saller *et al.*, 2008).

Two types of progradational stacking patterns have been identified at lobe scale due to limited lateral accommodation or an increase in sediment supply (Babonneau *et al.*, 2002; Picot *et al.*, 2016). Throughout the geological record, progradation has been defined

by vertical facies changes, *i.e.*, an increase in bed amalgamation, coarsening and thickening upward trends and erosive scours at lobe element scale (MacDonald *et al.*, 2011; Grundvåg *et al.*, 2014) and at lobe scale (Grundvåg *et al.*, 2014). Retrogradational stacking patterns may occur in two scenarios, due either to limited lateral accommodation, or reduction in sediment supply. Lobes in Rhone Neofan retrograde because of significant decrease in sediment supply (Jegou *et al.*, 2008).

Aggradational stacking patterns have been observed exclusively in confined systems (Eocene Hecho Group, Spain, in Remacha & Fernandez 2003; Miocene Marnoso-Arenacea Formation, Italy, in Talling, 2007 a, b; Amy & Talling, 2006; Oligocene Peira Cava, France, in Amy *et al.*, 2007; confined sheets of Lower Messinian Laga Basin, Italy, in Marini *et al.*, 2015). In an ideal aggradational stacking pattern, the maximum bed thicknesses remain constant, without any variation.

Facies associations

The identification of facies associations (*i.e.*, sub-environment) in turbidite sheet systems is mainly based on the degree of amalgamation and presence of associated lithofacies (Prélat *et al.*, 2009; Sychala *et al.*, 2017a). Four facies associations are commonly identified in

unconfined submarine lobes (Fig. 6). These are lobe axis-thick bedded highly amalgamated turbidite sandstone; lobe off axis-medium bedded structured turbidite sandstone; lobe fringe-thin bedded structured turbidite sandstone and lobe distal fringe-thin bedded siltstone.

In confined systems, only proximal and distal terminology have been used and differences are considerably smaller than those of unconfined turbidite sheet systems. The thinning rate of turbidite interval thickness ranges from 0.02 m/km to 0.2 m/km; decreasing rates of sand percentages range from 0.5%/km to 1%/km (Table 2). In the example of the Marnoso Arenacea Formation, Italy, only one facies association could be recognized with similar properties maintained across the basin (Fig. 6).

Onlap styles

Sedimentary features of fringe facies associations could be good indicators of the degree of confinement of turbidite systems (McCaffrey & Kneller, 2001; Smith & Joseph 2004; Spychala *et al.*, 2017b). Fringe facies associations change from ‘abrupt onlap fringes’ to ‘aggradational onlap fringes,’ then from ‘facies transitions fringes’ to

‘downlap fringes’ with decreasing confinement from high to low (Fig. 5; Spychala *et al.*, 2017b). ‘Facies transition fringes’ are represented by thinly-bedded, laminated to structureless siltstone and current/climbing ripple-laminated, very fine-grained sandstone.

Discussion

Sedimentary process

The sedimentary facies transitions from axis to margin are good indicators for sedimentary processes. In unconfined settings, flows either change from high-density turbidity currents to low density turbidity current due to flow non-uniformity or transition into laminar flow when the flows are mud-rich and finer grained. An ideal sedimentary facies model in a turbidite bed was proposed to include five types of sedimentary structure transitions name Ta-Te, *i.e.*, Ta graded interval to Tb lower parallel laminae, Tc current ripple laminae, Td upper parallel laminae and Te pelitic interval (Bouma *et al.*, 1964). When turbidity currents enter the basin floor from the channel mouth, they undergo rapid radial expansion with change of

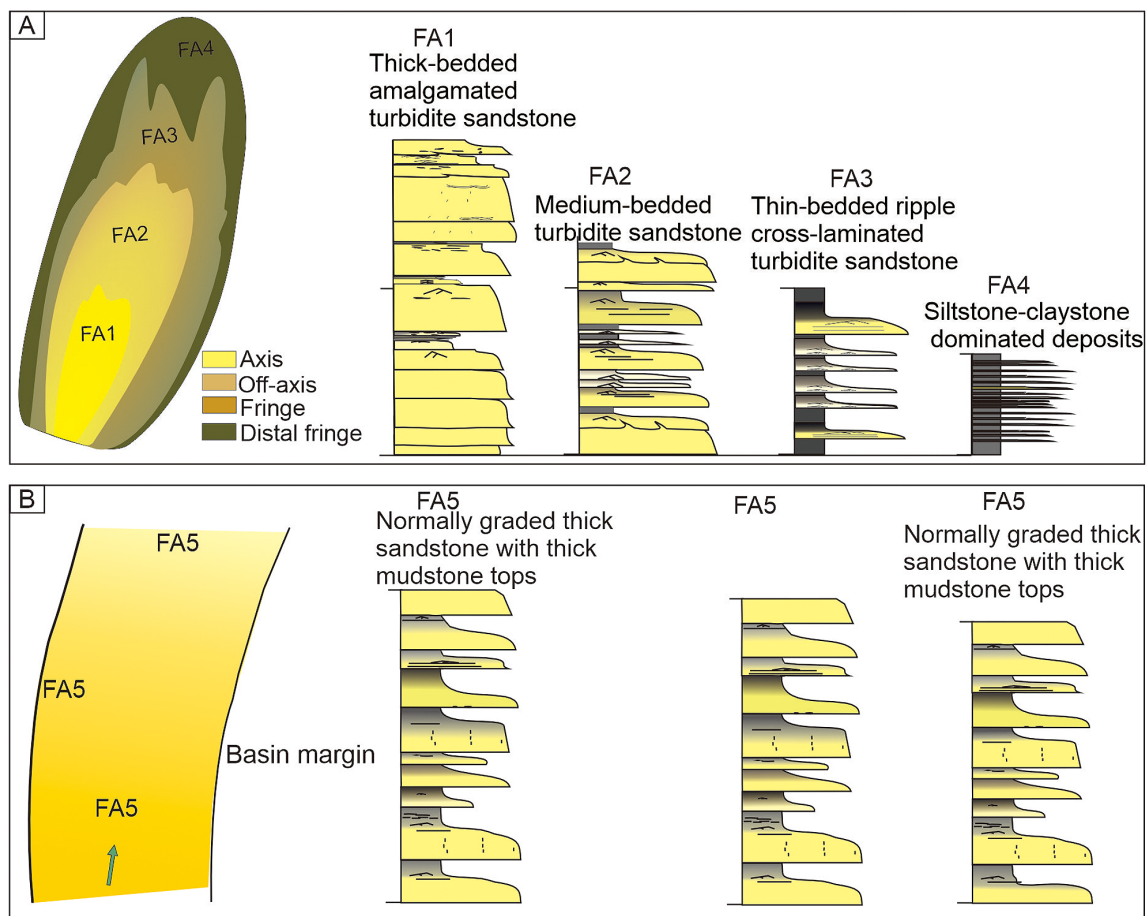


FIGURE 6. Lobe sub-environment with their representative facies associations. **A**, In unconfined systems, a transition occurs in the axial part to the distal part of a lobate depositional unit. **B**, In confined systems, no transition in facies association in depositional unit, only a slight decrease in total thickness.

TABLE 2. Summarized facies association characteristics of confined systems.

Studied intervals	Degree of confinement	Rate of facies associations change (Dip direction)	
		Thinning rate of turbidite interval thickness	Decreasing rate of sand percentage
Peira Cava, France (Amy <i>et al.</i> , 2007; McCaffrey & Kneller, 2001)	Lateral confinement	0.1 m/km	1% /km
Eocene Hecho Group, Spain (Remacha <i>et al.</i> , 2005)	Ponded	0.05 m/km	0.5% /km
'Confined lobes' of Lower Messinian Laga Basin (Marini <i>et al.</i> , 2015)	Confined	0.2 m/km	1% /km
Marnoso Arenacea, Italy (Amy & Talling, 2006)	Lateral confinement	0.02 m/km	0.5% /km

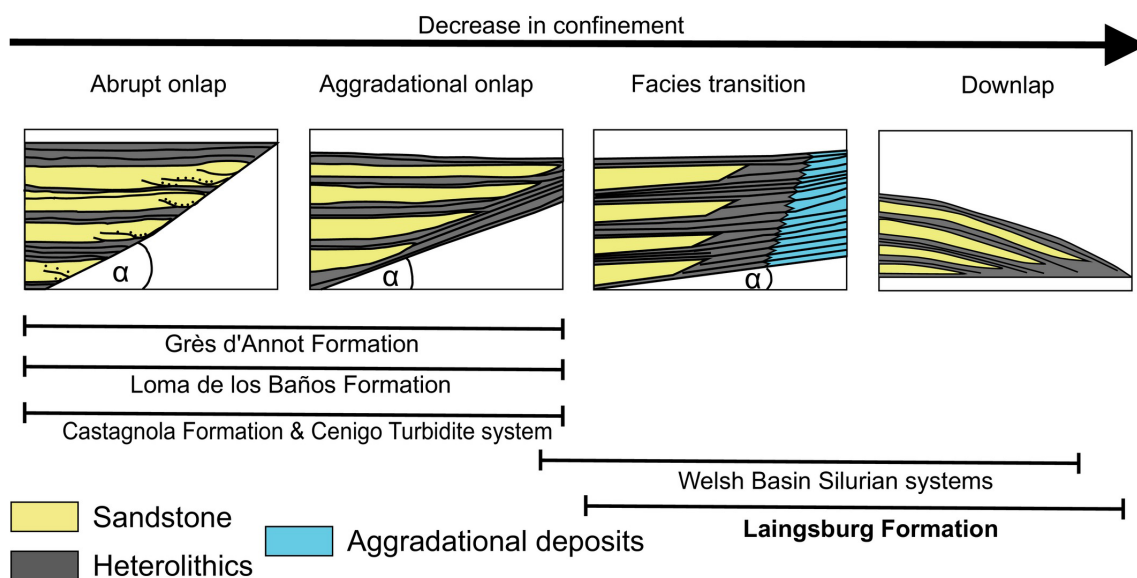


FIGURE 7. Fringe facies associations with different degrees of confinement. Abrupt onlap: low amount of aggradation on the slope, abrupt pinch out against structure. Aggradational onlap: moderate amount of aggradation on the slope compared to the basin, aggradational onlap with draping muds. Facies transitions: low-gradient slope and high aggradation rates, facies transition and remobilization (Spychala *et al.*, 2017b).

confinement and decrease in slope and are thus most likely to be depletive and waning flows, resulting in the rapid deposition of the remaining sediment, forming the normally graded sedimentary facies.

In confined systems, flows interact with basin slope by deflecting and reflecting from the basin margin (Kneller, 1995; Patacci *et al.*, 2015; Southern *et al.*, 2015). In highly ponded systems, flows 'slosh' back and forth in the basin several times until the energy is fully dissipated (Fig. 8; Pickering & Hiscott, 1985). A ponded suspension cloud of mud floccule may be established due to partial or complete trapping of turbulent currents (Patacci *et al.*, 2015; Lucchi & Valmori, 1980; Pickering & Hiscott, 1985), thus individual deposits would commonly have a thick mud cap.

Hierarchy of turbidite sheet systems

Various hierarchical schemes have been proposed to represent the different level of stacking patterns of unconfined turbidite sheet systems (Table 3; Gervais *et al.*, 2006; Deptuck *et al.*, 2008; Jegou *et al.*, 2008; Saller *et al.*, 2008; Prélat *et al.*, 2009; Mulder & Etienne, 2010; MacDonald *et al.*, 2011; Grundvåg *et al.*, 2014; Terlaky *et al.*, 2016). The hierarchical scheme proposed by Deptuck *et al.* and (2008) and Prélat *et al.* (2009) are widely accepted afterwards: 1) a 'bed' represents a single depositional event; 2) one or more beds stack to form a 'lobe element'; 3) several lobe elements that are divided by thin siltstone intervals form a 'lobe'; 4) one or more related lobes stack to form a 'lobe complex' (Fig. 9). The controlling factor on deposition of each hierarchical

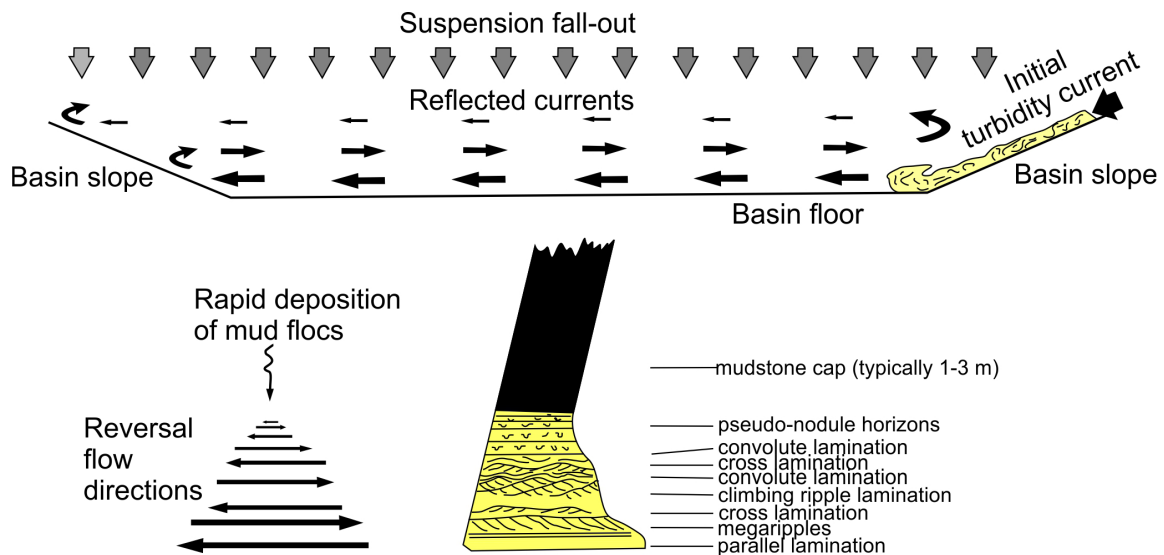


FIGURE 8. Origin of typical facies (F10) produced in confined turbidite sheet systems, which were produced by multiple deflections and reflections from basin margin slopes. Redrawn from Haughton (1994).

TABLE 3. Comparisons of hierarchies used to describe submarine lobe deposits in outcrop and geological studies.

Authors	Dataset	Hierarchy scheme proposed in unconfined turbidite sheet systems				
Prélat <i>et al.</i> , 2009	Outcrop	Bed/bedset	Lobe element	Lobe	Lobe complex	Lobe complex set
Grundvåg <i>et al.</i> , 2014						
Mulder & Etienne, 2010	Outcrop	Bed	Lobe element	Lobe	Lobe system	Lobe complex
Gervais <i>et al.</i> , 2006	Geophysical	Elementary sedimentary body		Internal unit	Lobe	Lobe complex
Deptuck <i>et al.</i> , 2008	Geophysical and outcrop	Bed	Lobe element	Composite lobe	Lobe complex	
MacDonald <i>et al.</i> , 2011						
Jegou <i>et al.</i> , 2008	Geophysical		Subunit	Channel-mouth lobe	Channel-mouth lobe complex	
Saller <i>et al.</i> , 2008	Geophysical		Sheetlike splay elements	Lobe	Fan	
Terlaky <i>et al.</i> , 2016	Outcrop	Bed	Architectural element	Lobe	Lobe complex	Fan

element is different: lobe elements are initiated by avulsion of distributary channels; lobes are initiated by avulsion of feeder channel; lobe complexes are initiated by avulsion of channel-levee system; and fans are initiated by avulsion of feeder canyons. Avulsions at the lowest levels in the hierarchy likely have an autogenic control and allogenic controls become more dominant at higher levels (Terlaky *et al.*, 2016).

No hierarchical scheme has been proposed for confined turbidite sheet systems (with confinement at the bed scale) (Mutti, 1977; Lucchi & Valmori, 1980; Pickering & Hiscott, 1985; Haughton, 1994; Wynn *et al.*, 2002; Remacha & Fernandez, 2003; Remacha *et al.*, 2005; Amy & Talling, 2006; Talling *et al.*, 2007a, b; Marini *et al.*,

2015; Fonnesu *et al.*, 2016; Muzzi Magalhaes & Tinterri, 2010). It is thus advocated here that the hierarchical scheme does not apply to confined systems and such terminology should be avoided in confined systems.

Allogenic and autogenic controls on unconfined and confined turbidite sheet systems

In confined turbidite sheet systems, individual turbidity currents are efficient enough to reach the basin margin and systems are built up by the vertical stacking of individual beds (Lucchi & Valmori, 1980; Weaver *et al.*, 1992; Wynn *et al.*, 2002; Remacha & Fernandez, 2003; Amy & Talling, 2006; Stevenson *et al.*, 2013). However, in unconfined turbidite sheet systems, individual turbidity

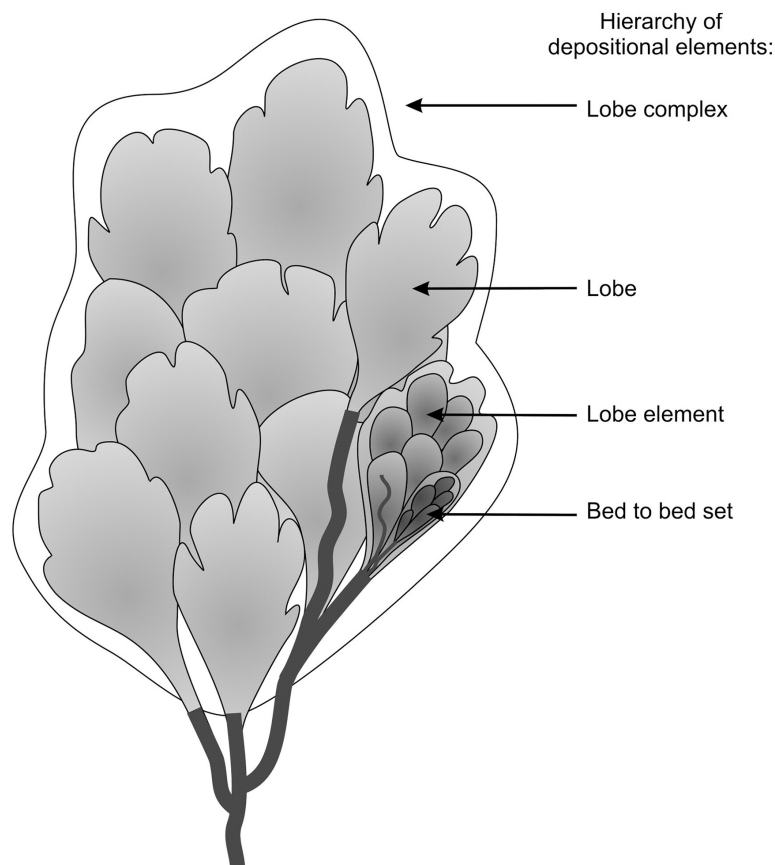


FIGURE 9. Schematic model of a fourfold hierarchical scheme proposed in unconfined turbidite sheet systems (Prélat *et al.*, 2010).

currents are not powerful enough to reach the basin margin and systems are built up by compensational stacking of individual beds (Dudley *et al.*, 2000; Prélat *et al.*, 2009; Marini *et al.*, 2015).

Depositional architectures of turbidite sheet systems are controlled by allogenic and autogenic factors (Prélat *et al.*, 2009, 2010; Groenenberg *et al.*, 2010; Cullis *et al.*, 2018). Allogenic controls include climate change, sea level fluctuation, and/or tectonic forcing (Cullis *et al.*, 2018; Terlaky *et al.*, 2016), which determine sediment supply and accommodation of the depositional systems. Autogenic controls include examples such as the frequency and occurrence of channel avulsion and depositional relief on the sea floor (Deptuck *et al.*, 2008; Terlaky *et al.*, 2016), which determine the auto-compensational style of the sand body.

It is found that both sediment supply and accommodation control the development of lobes (Fig. 10). Sediment supply is determined by climate, tectonic and sea level variations. Degree of confinement is determined by both the sediment supply (flow property) and local topography. Flows are unconfined and compensationally stack when sediment supply is small compared to basin size; flows are confined and vertically stack instead of compensating when sediment supply is large compared

to basin size. Prélat *et al.* (2009) and Terlaky *et al.* (2016) invoked internal factors as playing a dominant role below lobe complex level (terminology may vary between systems) and external factors are dominant above lobe complex level.

Conclusion

Turbidite sheet systems are a general term used to describe the deposits at the terminus of submarine channels, characterized by high aspect ratios. The depositional architecture of turbidite sheet systems is a key research area with not only scientific interesting but also economic importance. This study examines about twenty well-studied turbidite sheet systems to compare their sedimentary characteristics. At the two ends of the spectrum—confined and unconfined turbidite sheet systems—there are notable differences in sedimentary facies, stacking patterns, facies associations, and overall depositional architectures. These different parameters can serve as indicators of the degree of confinement, aiding in the prediction and understanding of an unknown turbidite sheet system.

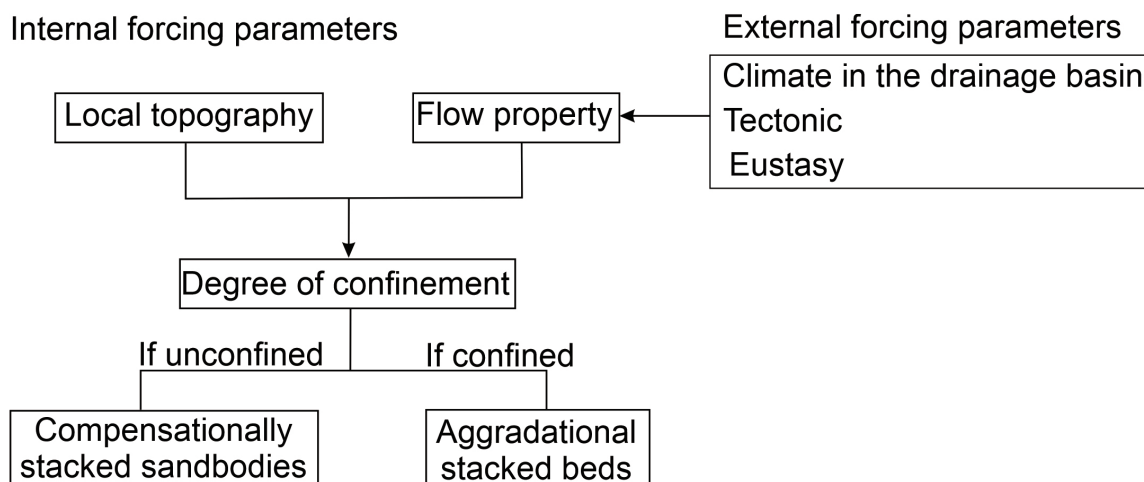


FIGURE 10. Summarized controlling factors of turbidite sheet systems (Jegou, 2008).

Acknowledgements

This work was financially supported by the National Natural Science Foundation of China (42002114), the Natural Science Foundation of the Jiangsu Higher Education Institutions of China (21KJB170014), and the Second Tibetan Plateau Scientific Expedition and Research Program (STEP, Grant No. 2019QZKK0204).

References

- Amy, L.A. & Talling, P.J. (2006) Anatomy of turbidites and linked debrites based on long distance (120× 30 km) bed correlation, Marnoso Arenacea Formation, Northern Apennines, Italy. *Sedimentology*, 53 (1), 161–212. <https://doi.org/10.1111/j.1365-3091.2005.00756.x>
- Amy, L.A., Kneller, B.C. & McCaffrey, W.D. (2007) Facies architecture of the Gres de Peira Cava, SE France: landward stacking patterns in ponded turbiditic basins. *Journal of the Geological Society*, 164, 143–162. <https://doi.org/10.1144/0016-76492005-019>
- Babonneau, N., Savoye, B., Cremer, M. & Klein, B. (2002) Morphology and architecture of the present canyon and channel system of the Zaire deep-sea fan. *Marine and Petroleum Geology*, 19, 445–467. [https://doi.org/10.1016/S0264-8172\(02\)00009-0](https://doi.org/10.1016/S0264-8172(02)00009-0)
- Bouma, A. (1964) Turbidites. 247–256. *In: Developments in sedimentology*, Elsevier (Vol. 3). [https://doi.org/10.1016/S0070-4571\(08\)70967-1](https://doi.org/10.1016/S0070-4571(08)70967-1)
- Cullis, S., Colombera, L., Patacci, M. & McCaffrey, W.D. (2018) Hierarchical classifications of the sedimentary architecture of deep-marine depositional systems. *Earth-Science Reviews*, 179, 38–71. <https://doi.org/10.1016/j.earscirev.2018.01.016>
- Deptuck, M.E., Piper, D.J., Savoye, B. & Gervais, A. (2008) Dimensions and architecture of late Pleistocene submarine lobes off the northern margin of East Corsica. *Sedimentology*, 55, 869–898. <https://doi.org/10.1111/j.1365-3091.2007.00926.x>
- Dudley, P.R., Rehmer, D.E. & Bouma, A.H. (2000) Reservoir-scale characteristics of fine-grained sheet sandstones, Tanqua Karoo Subbasin, South Africa. *In: Deep-Water Reservoirs of the World. SEPM, Gulf Coast Section, 20th Annual Research Conference, Houston, Texas*, 318–341. <https://doi.org/10.5724/gcs.00.15.0318>
- Gervais, A., Savoye, B., Mulder, T. & Gonthier, E. (2006) Sandy modern turbidite lobes: a new insight from high resolution seismic data. *Marine and Petroleum Geology*, 23, 485–502. <https://doi.org/10.1016/j.marpetgeo.2005.10.006>
- Groenenberg, R.M., Hodgson, D.M., Prelat, A., Luthi, S.M. & Flint, S.S. (2010) Flow-deposit interaction in submarine lobes: Insights from outcrop observations and realizations of a process-based numerical model. *Journal of Sedimentary Research*, 80, 252–267. <https://doi.org/10.2110/jsr.2010.028>
- Grundvåg, S.A., Johannessen, E.P., Helland-Hansen, W. & Plink-Björklund, P. (2014) Depositional architecture and evolution of progradationally stacked lobe complexes in the Eocene Central Basin of Spitsbergen. *Sedimentology*, 61, pp. 535–569. <https://doi.org/10.1111/sed.12067>
- Haughton, P.D. (1994) Deposits of deflected and ponded turbidity events, currents, Sorbas Basin, southeast Spain. *Journal of Sedimentary Research*, 64, 233–246. <https://doi.org/10.1306/D4267D6B-2B26-11D7-8648000102C1865D>
- Hodgson, D.M. & Haughton, P.D. (2004) Impact of syndepositional faulting on gravity current behaviour

- and deep-water stratigraphy: Tabernas-Sorbas Basin, SE Spain. In: Lomas, S.A. and Joseph, P. (Eds), Confined Turbidite Systems. *Geological Society of London, Special Publications*, 224, 135–158.
<https://doi.org/10.1144/GSL.SP.2004.222.01.05>
- Jegou, I., Savoye, B., Pirmez, C. & Droz, L. (2008) Channel-mouth lobe complex of the recent Amazon Fan: The missing piece. *Marine Geology*, 252, 62–77.
<https://doi.org/10.1016/j.margeo.2008.03.004>
- Kneller, B. (1995) Beyond the turbidite paradigm: physical models for deposition of turbidites and their implications for reservoir prediction. In: Hartley, A.J. & Prosser, D.J. (Eds), Characterization of deep marine clastic systems. *Geological Society of London, Special Publications*, 94, 31–49.
<https://doi.org/10.1144/GSL.SP.1995.094.01.04>
- Kneller, B., Nasr-Azadani, M. M., Radhakrishnan, S. & Meiburg, E. (2016) Long-range sediment transport in the world's oceans by stably stratified turbidity currents. *Journal of Geophysical Research: Oceans*, 121 (12), 8608–8620.
<https://doi.org/10.1002/2016JC011978>
- Liu, Q., Kneller, B., Fallgatter, C., Valdez Buso, V. & Milana, J.P. (2018a) Tabularity of individual turbidite beds controlled by flow efficiency and degree of confinement. *Sedimentology*, 65 (7), 2368–2387.
<https://doi.org/10.1111/sed.12470>
- Liu, Q., Kneller, B., Fallgatter, C. & Buso, V.V. (2018b) Quantitative comparisons of depositional architectures of unconfined and confined turbidite sheet systems. *Sedimentary Geology*, 376, 72–89.
<https://doi.org/10.1016/j.sedgeo.2018.08.005>
- Liu, Q., Kneller, B., An, W. & Hu, X. (2021) Sedimentological responses to initial continental collision: triggering of sand injection and onset of mass movement in a syn-collisional trench basin, Saga, southern Tibet. *Journal of the Geological Society*, 178 (6), jgs2020–178.
<https://doi.org/10.1144/jgs2020-178>
- Lucchi, F.R. & Valmori, E. (1980) Basin-wide turbidites in a Miocene, over-supplied deep-sea plain: a geometrical analysis. *Sedimentology*, 27, 241–270.
<https://doi.org/10.1111/j.1365-3091.1980.tb01177.x>
- Macdonald, H.A., Peakall, J., Wignall, P.B. & Best, J. (2011) Sedimentation in deep-sea lobe-elements: implications for the origin of thickening-upward sequences. *Journal of the Geological Society*, 168, 319–332.
<https://doi.org/10.1144/0016-76492010-036>
- Marini, M., Milli, S., Ravnås, R. & Moscatelli, M. (2015) A comparative study of confined vs. semi-confined turbidite lobes from the Lower Messinian Laga Basin (Central Apennines, Italy): Implications for assessment of reservoir architecture. *Marine and Petroleum Geology*, 63, 142–165.
<https://doi.org/10.1016/j.marpetgeo.2015.02.015>
- Meiburg, E. & Kneller, B. (2010) Turbidity currents and their deposits. *Annual Review of Fluid Mechanics*, 42, 135–156.
<https://doi.org/10.1146/annurev-fluid-121108-145618>
- McCaffrey, W. & Kneller, B. (2001) Process controls on the development of stratigraphic trap potential on the margins of confined turbidite systems and aids to reservoir evaluation. *AAPG Bulletin*, 85, 971–988.
<https://doi.org/10.1306/8626CA41-173B-11D7-8645000102C1865D>
- Mutti, E. (1977) Distinctive thin-bedded turbidite facies and related depositional environments in the Eocene Hecho Group (South-central Pyrenees, Spain). *Sedimentology*, 24, 107–131.
<https://doi.org/10.1111/j.1365-3091.1977.tb00122.x>
- Mutti, E. & Lucchi, F.R. (1978) Turbidites of the northern Apennines: introduction to facies analysis. *International Geology Review*, 20, 125–166.
<https://doi.org/10.1080/00206817809471524>
- Mutti, E. & Normark, W.R. (1987) Comparing examples of modern and ancient turbidite systems: problems and concepts. 1–38. In: Marine clastic sedimentology, Springer Netherlands.
https://doi.org/10.1007/978-94-009-3241-8_1
- Mutti, E. & Sonnino, M. (1981) Compensation cycles: a diagnostic feature of turbidite sandstone lobes. In International Association of Sedimentologists, 2nd European Regional Meeting, Bologna, 120–123.
- Normark, W.R. & Piper, D.J. (1991) Initiation processes and flow evolution of turbidity currents: implications for the depositional record. In: Osborne, R.H. (Eds), Shoreline to Abyss: Contributions in Marine Geology in Honor of Francis Parker Shepard. *SEPM Society for Sedimentary Geology*, 46, 207–230.
<https://doi.org/10.2110/pec.91.09.0207>
- Patacci, M., Haughton, P.D. & McCaffrey, W.D. (2015) Flow behavior of ponded turbidity currents. *Journal of Sedimentary Research*, 85, 885–902.
<https://doi.org/10.2110/jsr.2015.59>
- Pickering, K.T. & Hiscott, R.N. (1985) Contained (reflected) turbidity currents from the Middle Ordovician Cloridorme Formation, Quebec, Canada: an alternative to the antidune hypothesis. *Sedimentology*, 32, 373–394.
<https://doi.org/10.1111/j.1365-3091.1985.tb00518.x>
- Picot, M., Droz, L., Marsset, T., Dennielou, B. & Bez, M. (2016) Controls on turbidite sedimentation: insights from a quantitative approach of submarine channel and lobe architecture (Late Quaternary Congo Fan). *Marine and Petroleum Geology*, 72, 423–446.
<https://doi.org/10.1016/j.marpetgeo.2016.02.004>
- Prélat, A., Hodgson, D.M. & Flint, S.S. (2009) Evolution, architecture and hierarchy of distributary deep-water deposits: a high resolution outcrop investigation from the Permian Karoo Basin, South Africa. *Sedimentology*, 56, 2132–2154.
<https://doi.org/10.1111/j.1365-3091.2009.01073.x>
- Prélat, A., Covault, J.A., Hodgson, D.M., Fildani, A. & Flint, S.S. (2010) Intrinsic controls on the range of volumes, morphologies, and dimensions of submarine lobes. *Sedimentary Geology*, 232, 66–76.
<https://doi.org/10.1016/j.sedgeo.2010.09.010>

- Remacha, E. & Fernández, L.P. (2003) High-resolution correlation patterns in the turbidite systems of the Hecho Group (South-Central Pyrenees, Spain). *Marine and Petroleum Geology*, 20, 711–726.
<https://doi.org/10.1016/j.marpetgeo.2003.09.003>
- Remacha, E., Fernández, L.P. & Maestro, E. (2005) The transition between sheet-like lobe and basin-plain turbidites in the Hecho basin (south-central Pyrenees, Spain). *Journal of Sedimentary Research*, 75, 798–819.
<https://doi.org/10.2110/jsr.2005.064>
- Saller, A., Werner, K., Sugiaman, F., Cebastian, A., May, R., Glenn, D. & Barker, C. (2008) Characteristics of Pleistocene deep-water fan lobes and their application to an upper Miocene reservoir model, offshore East Kalimantan, Indonesia. *AAPG Bulletin*, 92, 919–949.
<https://doi.org/10.1306/03310807110>
- Smith, R. & Joseph, P. (2004) Onlap stratal architectures in the Gres d'Annot: geometric models and controlling factors. Geological Society, London, Special Publications, 221 (1), 389–399.
<https://doi.org/10.1144/GSL.SP.2004.221.01.21>
- Spychala, Y.T., Hodgson, D.M., Prélat, A., Kane, I.A., Flint, S.S. & Mountney, N.P. (2017a) Frontal and lateral submarine lobe fringes: comparing sedimentary facies, architecture and flow processes. *Journal of Sedimentary Research*, 87, 75–96.
<https://doi.org/10.2110/jsr.2017.2>
- Spychala, Y.T., Hodgson, D.M., Stevenson, C.J. & Flint, S.S. (2017b) Aggradational lobe fringes: The influence of subtle intrabasinal seabed topography on sediment gravity flow processes and lobe stacking patterns. *Sedimentology*, 64, 582–608.
<https://doi.org/10.1111/sed.12315>
- Southern, S.J., Patacci, M., Felletti, F. & McCaffrey, W.D. (2015) Influence of flow containment and substrate entrainment upon sandy hybrid event beds containing a co-genetic mud-clast-rich division. *Sedimentary Geology*, 321, 105–122.
<https://doi.org/10.1016/j.sedgeo.2015.03.006>
- Stevenson, C.J., Talling, P.J., Wynn, R.B., Masson, D.G., Hunt, J.E., Frenz, M., Akhmetzhanov, A. & Cronin, B.T. (2013) The flows that left no trace: Very large-volume turbidity currents that bypassed sediment through submarine channels without eroding the sea floor. *Marine and Petroleum Geology*, 41, 186–205.
<https://doi.org/10.1016/j.marpetgeo.2012.02.008>
- Talling, P.J., Amy, L.A., Wynn, R.B., Blackbourn, G. & Gibson, O. (2007a) Evolution of Turbidity Currents Deduced from Extensive Thin Turbidites: Marnoso Arenacea Formation (Miocene), Italian Apennines. *Journal of Sedimentary Research*, 77, 172–196.
<https://doi.org/10.2110/jsr.2007.018>
- Talling, P.J., Amy, L.A. & Wynn, R.B. (2007b) New insight into the evolution of large-volume turbidity currents: comparison of turbidite shape and previous modelling results. *Sedimentology*, 54, 73–769.
<https://doi.org/10.1111/j.1365-3091.2007.00858.x>
- Terlaky, V., Rocheleau, J. & Arnott, R.W.C. (2016) Stratal composition and stratigraphic organization of stratal elements in an ancient deep-marine basin-floor succession, Neoproterozoic Windermere Supergroup, British Columbia, Canada. *Sedimentology*, 63, 136–175.
<https://doi.org/10.1111/sed.12222>
- Tórkés, L. & Patacci, M. (2018) Quantifying tabularity of turbidite beds and its relationship to the inferred degree of basin confinement. *Marine and Petroleum Geology*, 97, 659–671.
<https://doi.org/10.1016/j.marpetgeo.2018.06.012>
- Weaver, P.P.E., Rothwell, R.G., Ebbing, J., Gunn, D. & Hunter, P.M. (1992) Correlation, frequency of emplacement and source directions of megaturbidites on the Madeira Abyssal Plain. *Marine Geology*, 109, 1–20.
[https://doi.org/10.1016/0025-3227\(92\)90218-7](https://doi.org/10.1016/0025-3227(92)90218-7)
- Wynn, R.B., Weaver, P.P., Masson, D.G. & Stow, D.A. (2002) Turbidite depositional architecture across three interconnected deep-water basins on the north-west African margin. *Sedimentology*, 49, 669–695.
<https://doi.org/10.1046/j.1365-3091.2002.00471.x>